RESEARCH ARTICLE

NANO · MICRO small
www.small-journal.com

Consecutive Complex Aggregation Pathway in Covalent Helical Polymer-Metal Complexes: Nanospheres with Controlled *P*/*M* Macroscopic Chirality

*Juan José Tarrío, Borja Hermida, Rafael Rodríguez, Jeanne Crassous, Emilio Quiñoá, and Félix Freire**

Kinetically trapped and thermodynamic nanospheres with opposite macroscopic *P*/*M* chirality and opposite circularly polarized luminescence (CPL) can be obtained from a single helical polymer-metal complex under the same environmental conditions. To prepare these nanospheres, a chiral poly(diphenylacetylene) (PDPA) [poly-(*L*)-1] with a large energy barrier between the *P* and *M* helical senses is chosen as source of chirality, while Ba^{2+} metal ions are selected as crosslinking agents. As a result, the poly-(*L*)-1/Ba^{2+} complex can generate both kinetically trapped (Agg_1, *M* nanospheres) and thermodynamic (Agg_2, *P* nanospheres) aggregates, which can be dispersed in the same solvent. Due to the high energy barrier of the helix inversion process for poly-(*L*)-1, the complete evolution from the kinetically trapped aggregate (Agg_1, *M* nanospheres) to the thermodynamic one (Agg_2, *P* nanospheres) takes more than 75 days at room temperature, which can be accelerated at higher temperatures. These nanospheres are stable and remain dispersed in solution for up to 8 months without further aggregation.

1. Introduction

Macroscopically chiral aggregates such as fibers, nanospheres, micelles, or similar structures are usually obtained from the self-assembly of small molecules, which is driven by the presence of supramolecular interactions such as Van der Waals forces, dipole–dipole, hydrogen bonds or π–π interactions, among others.[1–6] To tune the macroscopic *P*/*M* chirality of supramolecular aggregates it is usually necessary to change the aggregate preparation protocol (solvent, temperature, additives), which alters the initial environmental conditions and can also change the morphology of the aggregate.[1–6] In some examples, opposite *P* and *M* chiralities can be obtained under the same environmental conditions when the aggregate is formed via a consecutive supramolecular polymerization mechanism.[7–13] In these cases, to keep the kinetic aggregate stable over time, it is necessary to trap it kinetically by altering the aggregation conditions (solvent, seeds).[14–22]

Dynamic helical polymers such as poly(phenylacetylene)s (PPAs)[23–37] have also been used to create chiral aggregates[14,38,39] by using metal ions as crosslinking agents[39–43] or solvent-assisted methods such as nanoprecipitation.[44] In both cases, tuning the macroscopic chirality of the polymer particle requires the addition of an external stimulus, which changes the initial conditions under which the chiral particles were prepared. Moreover, PPAs are light-sensitive, undergoing a photochemical electrocyclization reaction of the polyene backbone upon exposure to light, which breaks down the material and limits its potential use.[45,46]

In this work, we aim to overcome the stability problem associated with PPA/M^{n+} complexes and introduce new features into chiral nanospheres, such as the chiral memory effect or circularly polarized luminescence (CPL) emission. For this purpose, chiral poly(diphenylacetylene)s (PDPAs) were chosen as polymeric platforms, which exhibit a kinetically controlled dynamic helical behavior.[47,48] In these polymers, the two *P*/*M* screw-senses of the helix can be induced by playing with the conformational composition of the chiral pendant group at high temperatures.[49,50] Temperature provides the system with the energy required to

J. J. Tarrío, B. Hermida, E. Quiñoá, F. Freire
Centro Singular de investigación en Química Biolóxica e Materiais Moleculares (CiQUS) and Departamento de Química Orgánica
Universidade de Santiago de Compostela
Santiago de Compostela E-15782, Spain
E-mail: felix.freire@usc.es, felixmanuel.freire@uvigo.gal

R. Rodríguez, F. Freire
CINBIO
Departamento de Química Orgánica
Universidade de Vigo
Campus Universitario Lagoas Marcosende
Vigo 36310, Spain

J. Crassous
Univ Rennes
CNRS
ISCR (Institut des Sciences Chimiques de Rennes)
CNRS
UMR 6226, Rennes F-35000, France

The ORCID identification number(s) for the author(s) of this article can be found under https://doi.org/10.1002/smll.202409379

DOI: 10.1002/smll.202409379

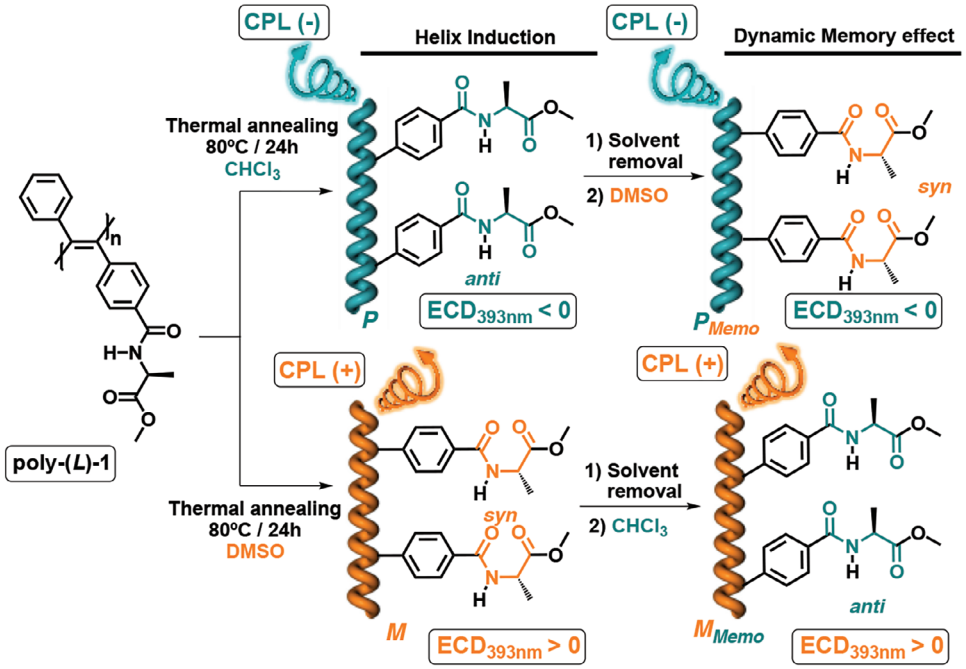

Figure 1. Chemical structure of poly-(*L*)-**1** and helix induction toward the *P* and *M* helical sense after thermal annealing in non-donor and donor solvents respectively. The dynamic memory effect produced after solvent removal and re-dissolution is also illustrated.

overcome the high energy barrier between the *P*/*M* helix orientations that is associated with steric effects in the PDPA backbone. This fact allows to kinetically trap the excess screw-sense once the external stimulus is removed.[50]

Thus, we hypothesize that if the dynamic memory effect of PDPA persists after complexation with metal ions, and if it is possible to control the aggregation of the resulting helical polymer-metal complex (HPMC) by controlling the polymer/M^{n+} ratio, it will be possible to create a kinetically trapped aggregate (Agg_1) that evolves toward the thermodynamic one (Agg_2), following a consecutive mechanism through a gradual helical inversion of PDPA within the aggregate.

2. Results and Discussion

To carry out these studies, an asymmetric PDPA bearing the 4-benzamide of (*L*)-alanine methyl ester as a pendant group in one of the aryl rings was chosen as a model compound [poly-(*L*)-**1**].[49,50] This polymer can adopt either *M* or *P* screw-sense excess in the polyene backbone (helix 1) after a thermal annealing (80 °C/24 h) in donor (dimethylformamide (DMF), dimethylsulfoxide (DMSO), tetrahydrofurane (THF), dioxane, acetone) and non-donor or very weak donor (1,2-dichloroethane (DCE), chloroform ($CHCl_3$), dichloromethane (CH_2Cl_2), and acetonitrile (MeCN)) solvents, respectively (**Figure 1**). The different helical sense adopted by poly-(*L*)-**1** in donor (*M* helix) and non-donor (*P* helix) solvents is attributed to a conformational change in the pendant groups inferred from vibrational circular dichroism (VCD) studies.[49,50] Thus, while in donor solvents the two carbonyl groups in the pendant (amide and ester) are oriented *synperiplanar* (*syn* conformation), in non-donor solvents these two carbonyls are positioned a*ntiperiplanar* (*anti* conformation) (Figure 1). As a result, chiroptical and CPL switches were obtained based on the donor character of the solvent. Interestingly, the helical sense adopted by poly-(*L*)-**1** after thermal annealing can be memorized, remaining unaltered after removal of the solvent, and being redissolved again in a new solvent with opposite donor character (Figure 1).

Hence, poly-(*L*)-**1** (0.5 mg mL^{-1}) was pre-annealed in 1,2-dichloroethane (DCE) and tetrahydrofuran (THF) at 80 °C for 24 h to induce a P_{helix} [DCE, pendant *syn* conformer, negative ECD band at 393 nm corresponding to the orientation of the PDPA backbone ($ECD_{393} < 0$)] and an M_{helix} (THF, pendant *anti* conformer, $ECD_{393} > 0$) in the PDPA (**Figure 2a**). The solvent was removed, and the helical sense was memorized in the solid state. The pre-oriented *P* and *M* screw-sense helices of poly-(*L*)-**1** were redissolved in a DCE/methanol (MeOH) (9/1 v/v) mixture, yielding the two orientations of the helix (P_{Memo} and M_{Memo}) for poly-(*L*)-**1** in the same solvent (DCE) (Figure 2b,c). MeOH was added to DCE as a cosolvent because it is necessary to deliver the metal salt to form the HPMC. Interestingly, although the preferred screw-sense for poly-(*L*)-**1** in DCE is the *P* helix (thermodynamic helix), the memorized *M* helical structure (M_{Memo} kinetic helix) induced in THF can remain in the DCE/MeOH mixture for more than 7 days (M_{Memo}), due to the high helix inversion barrier of the PDPA backbone (see ECD studies in Figure 2b). The complete helix inversion from the M_{Memo} (kinetic) toward the *P* helix (thermodynamic) for poly-(*L*)-**1** takes more than 75 days.

Thus, we explore the ability of poly-(*L*)-**1** to form nanospheres in the presence of metal ions, and the possibility of generating the two macroscopic *P* (thermodynamic) and *M* (kinetic) nanosphere enantiomers under the same experimental conditions.

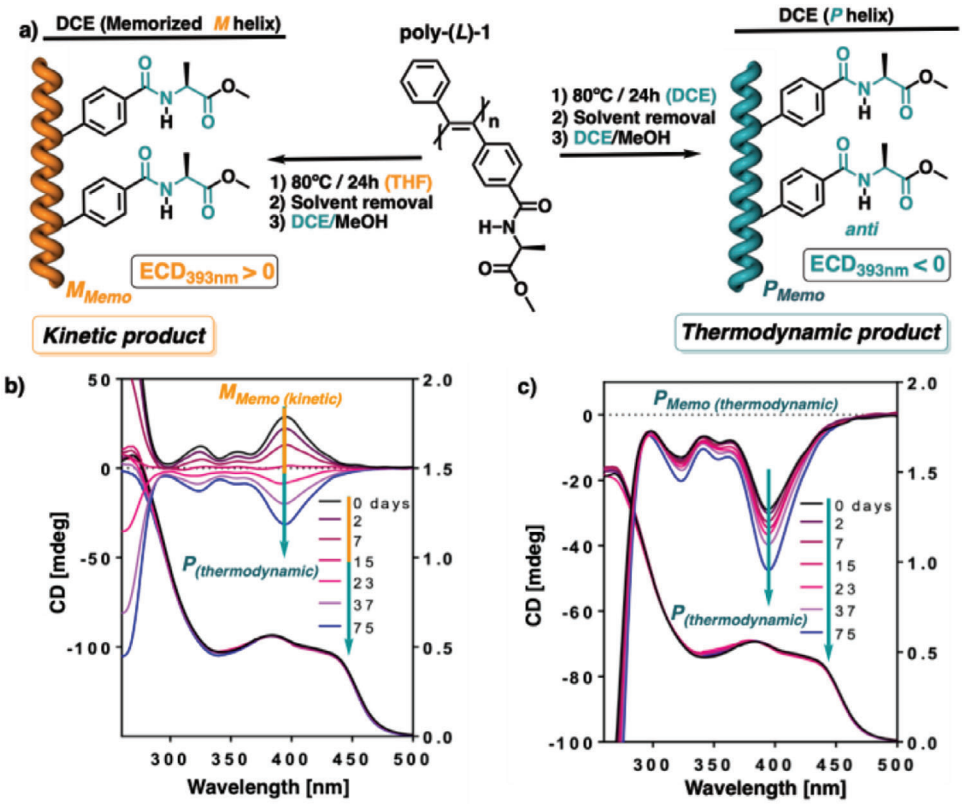

Figure 2. a) Schematic illustration of the preparation of the pre-oriented P_{Memo} and M_{Memo} helical scaffolds of poly-(*L*)-**1** and their dissolution in a DCE/MeOH mixture. b) Time evolution of the ECD spectra upon addition of MeOH to the M_{Memo} and P_{Memo} helical poly-(*L*)-**1** DCE solutions monitored by ECD. [poly-(*L*)-**1**] = 0.5 mg mL^{-1} DCE; MeOH 100µL mL^{-1} DCE.

Thus, perchlorate metal salts —$LiClO_4$ and $Ba(ClO_4)_2$— dissolved in MeOH (10 mg/mL) were then added to vials containing DCE solutions of poly-(*L*)-**1** (0.5 mg mL^{-1} DCE) folded into either a P_{Memo} or an M_{Memo} helix to generate a poly-(*L*)-**1**/M^{n+} complex at a monomer repeating unit (m.r.u.)/metal ratio of 1/2 mol/mol (**Figure** 3a,c). Infrared spectroscopy (IR) Ele studies show coordination of metal ions with the carbonyl groups at the pendant to form HPMCs (Figure S21, Supporting Information).

Dynamic light scattering (DLS) (Figure 3e) and surface electron microscopy (SEM) studies (Figure 3f,g) for the poly-(*L*)-**1** m.r.u./Mn^+ (Mn^+ = Li^+, Ba^{2+}) complexes at a 1/2 mol/mol ratio show the formation of spherical aggregates. Furthermore, from these studies, it was found that poly-(*L*)-**1**/Li^+ complexes produce polydisperse particles (Figure S16, Supporting Information), while poly-(*L*)-**1**/Ba^{2+} complexes produced nanospheres with a low polydispersity index (PDI) that remain unaltered over time (up to 8 months) (see Figure 3e–g for poly-(*L*)-**1**/Ba^{2+} and Figure S17 (Supporting Information) for poly-(*L*)-**1**/Li^+). IR studies show that while Li^+ ions coordinate only the carbonyl of the ester group, Ba^{2+} ions coordinate both the amide carbonyl and the ester carbonyl separately (Figure S16, Supporting Information).

So, while in poly-(*L*)-1/Li^+ complexes the metal ion is positioned toward the outer part of the helix, in the case of poly-(*L*)-1/Ba^{2+} complexes the metal ion is distributed between two different positions in the PDPA helical scaffold (inner and outer part). As a result, the metal ion is more prone to aggregate in poly-(*L*)-1/Li^+ complexes than in poly-(*L*)-1/Ba^{2+} complexes, making it difficult to control the polydispersity of the nanostructures. Thus, to study macroscopic dynamic *P*/*M* chirality through kinetic and thermodynamic aggregate formation, we focused our attention on poly-(*L*)-**1**/Ba^{2+} complexes and their corresponding aggregates.

Electronic circular dichroism (ECD) studies of poly-(*L*)-**1** m.r.u/Ba^{2+} HPMCs at a 1/2 mol/mol ratio showed that during the first few days (0 to 7 days), the pre-annealed P_{Memo} and M_{Memo} helical senses induced in poly-(*L*)-**1** are retained after metal ion complexation (Figure 3b,d). However, after 7 days, an evolution of the ECD spectra was observed in HPMCs containing both the pre-annealed P_{Memo} and M_{Memo} helices for poly-(*L*)-**1** (Figure 3b,d). Thus, vials containing poly-(*L*)-**1** folded into a P_{Memo} helix show an increase in the screw-sense excess — ECD enhancement— due to a further stabilization of the *anti*-conformation at the pendant group by metal ion complexation (Figure 3d).

On the contrary, vials containing poly-(*L*)-**1** folded into an M_{Memo} helix ($ECD_{393} > 0$) show a decrease in the *M* screw-sense excess, which evolves toward a *P* helical structure ($ECD_{393} < 0$). This effect is a consequence of a slow helix inversion process due to the stabilization of the *anti*-conformation in the pendant by metal ion complexation (Figure 3c). These results are similar to those previously obtained for the evolution of poly-(*L*)-**1**

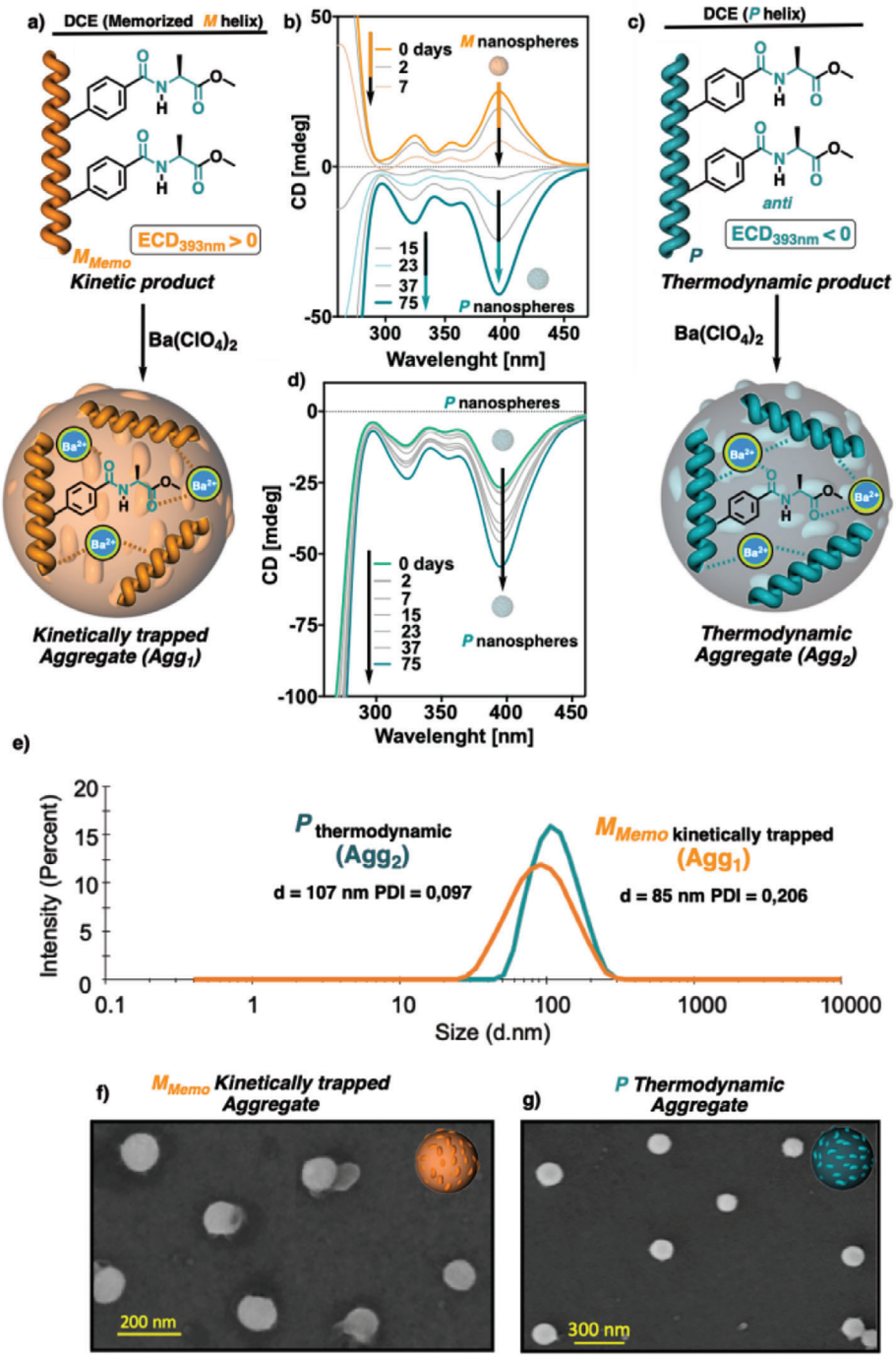

Figure 3. a) Schematic illustration for the preparation of kinetically trapped *M* chiral nanospheres (Agg_1). b) Time evolution of the pre-annealed M_{Memo} helix (kinetic helix) toward the *P* helix (thermodynamic helix) upon the addition 2.0 equiv of $Ba(ClO_4)_2$. c) Schematic illustration for the preparation of thermodynamic *P* oriented nanospheres (Agg_2). d) Time evolution of the pre-annealed P_{Memo} helix (thermodynamic helix) upon the addition 2.0 equiv of $Ba(ClO_4)_2$. e) DLS studies of the poly-(*L*)-**1**/Ba^{2+} kinetically trapped and thermodynamic aggregates. f) SEM image of the kinetically trapped poly-(*L*)-**1**/Ba^{2+} complex (Agg_1). g) SEM image of the thermodynamic poly-(*L*)-**1**/Ba^{2+} complex (Agg_2).

(M_{Memo} and P_{Memo}) in a DCE/MeOH mixture, without the presence of metal ions (Figure 2).

To determine whether metal ion coordination affects the kinetics of the helix inversion process for poly-(*L*)-**1**, time-dependent ECD studies were performed at different temperatures for a DCE solution of poly-(*L*)-**1** (M_{Memo}) (0.5 mg mL^{-1} DCE) treated with MeOH (100 µL of MeOH mL^{-1} DCE) and for a DCE/MeOH solution of poly-(*L*)-**1** m.r.u. (M_{Memo})/Ba^{2+} (1/2 mol/mol) —poly-(*L*)-**1** (0.5 mg mL^{-1} DCE); [$Ba(ClO_4)_2$] = 10 mg mL^{-1} MeOH— (Figure 2b,c and Supporting Information). These studies reveal

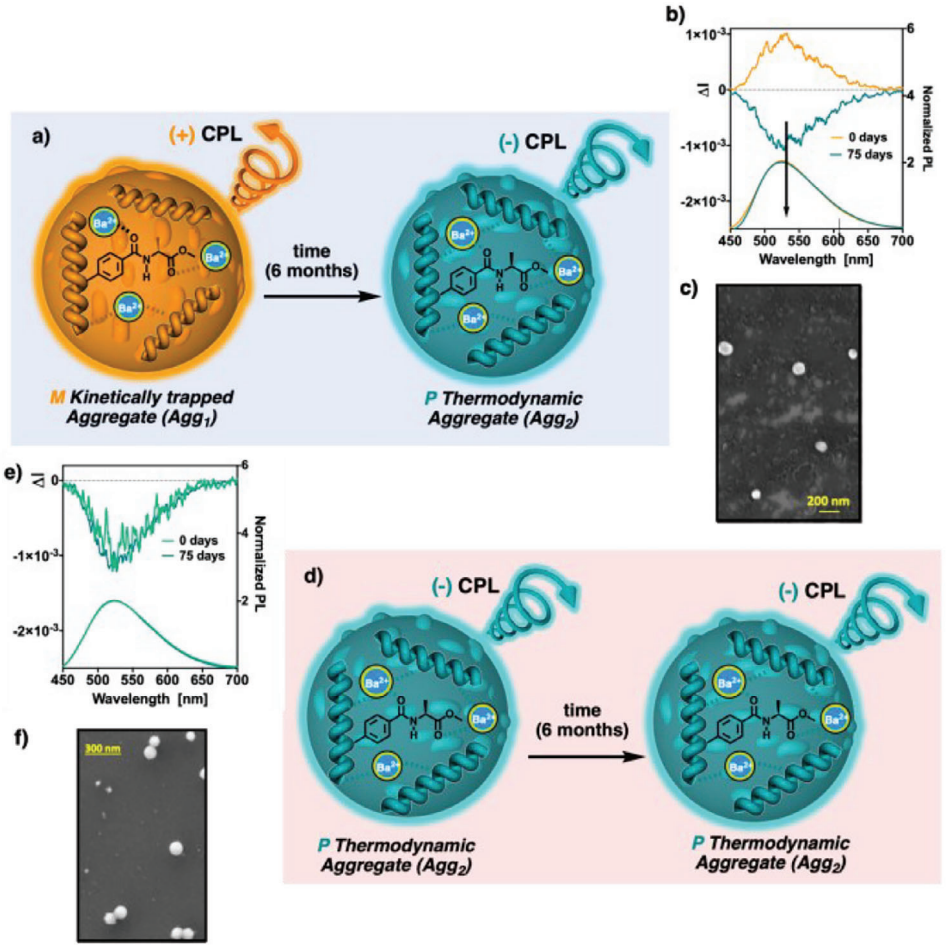

Figure 4. Schematic illustration of the time evolution for a) M_{Memo} Agg_1 and d) P_{Memo} Agg_2 obtained from poly-(*L*)-**1**/Ba^{2+} in DCE. CPL spectra of b) kinetically trapped [(M_{Memo})-Agg_1] and e) thermodynamic [(P_{Memo})-Agg_2] aggregates as prepared and after 75 days. SEM studies of (*P*)-Agg_2 from dispersions of c) kinetically trapped and f) thermodynamic aggregates allowed to evolve over time for 8 months.

similar kinetics for the M_{Memo} to *P* helix inversion process in a DCE solution of poly-(*L*)-**1** in the absence or presence of MeOH — activation energy (E_a) poly-(*L*)-**1** = 18.3 Kcal mol^{-1}, E_a poly-(*L*)-**1** (MeOH) = 16.0 Kcal mol^{-1}) (see Figures S13–S17, Supporting Information). However, an increase in the E_a of the M_{Memo} to *P* helix inversion process is observed in the poly-(*L*)-**1**/Ba^{2+} complex (E_a poly-(*L*)-**1**/Ba^{2+} = 30.1 Kcal mol^{-1}, Figures S16 and S17, Supporting Information). This fact indicates that the M_{Memo} to *P* helix inversion is occurring within the nanosphere, where the confinement and cross-linking ability of the metal ions explains the higher E_a of the helix inversion process in the presence of metal ions.

Time-dependent ECD, DLS and SEM studies show that while *P* aggregates of poly-(*L*)-**1**/Ba^{2+} (Agg1, $ECD_{393} < 0$) remain stable in DCE for more than 8 months (Figure 3c,d), *M* aggregates ($ECD_{393} > 0$) do not. In this case, a consecutive aggregation pathway is observed,[51–53] where a *P* aggregate (Agg_1) transforms into an *M* aggregate (Agg2) over time as monitored by ECD (Figure 3a,b,e–g). From VT-ECD studies and DLS experiments, we could observe that the nanospheres remain stable up to 343 K while the helix inversion accelerates (Figure S23, Supporting Information). Above this temperature, the nanospheres are not stable and precipitate due to the formation of large aggregates.

From the literature, it is known that PDPAs result in CPL-active materials once a screw-sense excess is induced in the polymer.[54,55] The sign of the CPL signal coincides with that of the high-energy band in the ECD spectra, which is associated with the helical sense of the polymer. Therefore, when ECD_{393} is negative (*P* helix), CPL should be negative and when the ECD_{393} is positive (*M* helix), CPL should be positive. Consequently, CPL studies were carried out for Agg1 [*M* nanospheres, $ECD_{393} > 0$] and Agg_2 [*P* nanospheres, $ECD_{393} < 0$] of the poly-(*L*)-**1**/Ba^{2+} complex (**Figure 4**). As expected, a positive CPL signal was obtained for Agg_1 (Figure 4b), while Agg_2 produced a negative one (Figure 4g).

The CPL emission was gauged by the dissymmetric factor defined as $|g_{lum}| = 2(I_L - I_R)/(I_L + I_R)$, where I_L and I_R are the left- and right-handed luminescent emissions respectively. In both cases, a maximum g_{lum} value of ca. $\pm 1.1 \times 10^{-3}$ was obtained at 520 nm, with quantum yield values of $\phi = 26$ and of $\phi = 44$ for the Agg_1 and Agg_2 solutions respectively. Interestingly, when the macroscopic chirality of the kinetic trap (Agg_1, M_{Memo}) evolves with time toward the enantiomeric form (thermodynamic

aggregate, Agg_2, P_{helix}), an opposite CPL emission is obtained. Thus, starting from a single HPMC, nanospheres with opposite CPL emission can be obtained by controlling the kinetics associated with the helix inversion effect of the polymer chain.

3. Conclusion

In conclusion, we have demonstrated that nanospheres with opposite macroscopic *P* or *M* axial chirality can be obtained from a PDPA/$Ba(ClO_4)_2$ system, following consecutive aggregation pathways. This fact is possible due to the high energy barrier of the helix inversion process intrinsic to the PDPA scaffold. Thus, a kinetic aggregate (Agg_1) can be trapped for days or even months at low temperatures and can evolve to a thermodynamic aggregate (Agg_2) through a consecutive aggregation mechanism. Interestingly, other properties associated with the chiral content of the aggregate, such as CPL, change once the PDPA helix is inverted within the aggregate.

The generation of these smart chiral polymeric particles, whose macroscopic chirality can be memorized or gradually evolved toward the opposite screw-sense, opens the door to the creation of supramolecular assemblies with controlled and tunable chiral cores and surfaces with potential applications in molecular recognition, information encryption or asymmetric synthesis, among others.

Supporting Information

Supporting Information is available from the Wiley Online Library or from the author.

Acknowledgements

The authors thank Servicio de Microscopía Electrónica (RIAIDT, USC). Financial support from AEI (PID2022-136848NB-I00), E.Q. and F.F.; Ramón y Cajal contract RYC2022-035587-I, R.R.), Xunta de Galicia (ED431C 2022/21, Centro Singular de Investigación de Galicia acreditación 2023–2027, ED431G 2023/03, ED431G 2023/06) and the European Regional Development Fund (ERDF) are gratefully acknowledged. J.J.T. thanks MICINN for a FPU contract. Funding for open access charge: Universidade de Vigo/CISUG.

Conflict of Interest

Inclusion of this piece of research in the thesis of the first author's dissertation.

Data Availability Statement

The data that support the findings of this study are available in the supplementary material of this article.

Keywords

chirality, CPL, dynamic macroscopic, helical polymer-metal complexes, nanospheres consecutive mechanism

Received: October 11, 2024
Revised: December 12, 2024
Published online: December 29, 2024

[1] M. Lago-Silva, M. Fernández-Míguez, R. Rodríguez, E. Quiñoá, F. Freire, *Chem. Soc. Rev.* **2024**, *53*, 793.
[2] Z. Fernández, L. Sánchez, S. Santhosh Babu, G. Fernández, *Angew. Chem., Int. Ed.* **2024**, *63*, 202402259.
[3] E. Yashima, N. Ousaka, D. Taura, K. Shimomura, T. Ikai, K. Maeda, *Chem. Rev.* **2016**, *116*, 13752.
[4] O. J. G. M. Goor, S. I. S. Hendrikse, P. Y. W. Dankers, E. W. Meijer, *Chem. Soc. Rev.* **2017**, *46*, 6621.
[5] M. Liu, L. Zhang, T. Wang, *Chem. Rev.* **2015**, *115*, 7304.
[6] L. Zhang, H.-X. Wang, S. Li, M. Liu, *Chem. Soc. Rev.* **2020**, *49*, 9095.
[7] J. Matern, K. K. Kartha, L. Sánchez, G. Fernández, *Chem. Sci.* **2020**, *11*, 6780.
[8] N. Bäumer, J. Matern, G. Fernández, *Chem. Sci.* **2021**, *12*, 12248.
[9] P. Khanra, A. K. Singh, L. Roy, A. Das, *J. Am. Chem. Soc.* **2023**, *145*, 5270.
[10] L. Borsdorf, L. Herkert, N. Bäumer, L. Rubert, B. Soberats, P. A. Korevaar, C. Bourque, C. Gatsogiannis, G. Fernández, *J. Am. Chem. Soc.* **2023**, *145*, 8882.
[11] Z. Fernández, B. Fernández, E. Quiñoá, F. Freire, *Angew. Chem., Int. Ed.* **2021**, *133*, 10007.
[12] M. A. Martínez, E. E. Greciano, L. Sánchez, *Chem. Eur. J.* **2019**, *25*, 16012.
[13] E. E. Greciano, R. Rodríguez, K. Maeda, L. Sánchez, *Chem. Commun.* **2020**, *56*, 2244.
[14] Y. Ji, K. Yang, B. Zhao, K. Pan, J. Deng, *ACS Macro Lett.* **2024**, *13*, 673.
[15] S. Ogi, K. Sugiyasu, S. Manna, S. Samitsu, M. Takeuchi, *Nat. Chem.* **2014**, *6*, 188.
[16] S. Kotha, R. Sahu, A. C. Yadav, P. Sharma, B. V. V. S. P. Kumar, S. K. Reddy, K. V. Rao, *Nat. Commun.* **2024**, *15*, 3672.
[17] E. E. Greciano, J. Calbo, E. Ortí, L. Sánchez, *Angew. Chem., Int. Ed.* **2020**, *59*, 17517.
[18] M. Wehner, M. I. S. Röhr, M. Bühler, V. Stepanenko, W. Wagner, F. Würthner, *J. Am. Chem. Soc.* **2019**, *141*, 6092.
[19] W. Wagner, M. Wehner, V. Stepanenko, F. Würthner, *J. Am. Chem. Soc.* **2019**, *141*, 12044.
[20] S. Patra, S. Chandrabhas, S. Dhiman, S. J. George, *J. Am. Chem. Soc.* **2024**, *146*, 12577.
[21] S. Sarkar, A. Sarkar, S. J. George, *Angew. Chem., Int. Ed.* **2020**, *59*, 19841.
[22] H. Itabashi, K. Tashiro, S. Koshikawa, S. Datta, S. Yagai, *Chem. Commun.* **2023**, *59*, 7375.
[23] E. Yashima, K. Maeda, H. Iida, Y. Furusho, K. Nagai, *Chem. Rev.* **2009**, *109*, 6102.
[24] J. W. Y. Lam, B. Z. Tang, *Acc. Chem. Res.* **2005**, *38*, 745.
[25] J. Liu, J. W. Y. Lam, B. Z. Tang, *Chem. Rev.* **2009**, *109*, 5799.
[26] X. Wan, H. Zeng, P. Yu, J. Zhang, *Angew. Chem., Int. Ed.* **2024**, *63*, 202417792.
[27] Y. Wang, X. Zhang, C.-B. Huang, L. Hu, X.-Q. Wang, W. Wang, H.-B. Yang, *Angew. Chem., Int. Ed.* **2024**, *63*, 202408271.
[28] E. Suarez-Picado, E. Quiñoá, R. Riguera, F. Freire, *Angew. Chem., Int. Ed.* **2020**, *59*, 4537.
[29] K. Cobos, R. Rodríguez, E. Quiñoá, R. Riguera, F. Freire, *Angew. Chem., Int. Ed.* **2020**, *59*, 23724.
[30] M. Lago-Silva, M. M. Cid, E. Quiñoá, F. Freire, *J. Am. Chem. Soc.* **2024**, *146*, 752
[31] L. Ren, X. Lu, W. Li, J. Yan, A. K. Whittaker, A. Zhang, *J. Am. Chem. Soc.* **2023**, *145*, 24906.
[32] X. Lu, Y. Liu, D. Lu, A. Xu, Y. Cao, X. Zhang, W. Li, A. Zhang, *Macromolecules* **2023**, *56*, 10206.
[33] F. Rey- Tarrío, E. Quiñoá, G. Fernández, F. Freire, *Nat. Chem.* **2023**, *14*, 3348.
[34] Y. Nishikawa, D. Hirose, S. Sona, K. Maeda, *Chem. Commun.* **2023**,*59*, 8226.

[35] C. Xu, S. Huang, S. Narita, M. Shibata, N. Nagaoka, M. Teraguchi, T. Kaneko, T. Aoki, *Macromolecules* **2023**, *56*, 3334.
[36] S. Wang, S. Xie, H. Du, J. Zeng, J. Zhang, J. Wan, *Sci. China Chem.* **2023**, *66*, 887.
[37] S. Cai, Y. Huang, S. Xie, S. Wang, Y. Guan, X. Wan, J. Zhang, *Angew. Chem., Int. Ed.* **2022**, *61*, 202214293.
[38] L. Shen, Y. Cao, L. Wang, X. Zhang, A. Zhang, W. Li, *Angew. Chem., Int. Ed.* **2024**, *63*, 202407552.
[39] S. Arias, M. Núñez-Martínez, E. Quiñoá, R. Riguera, F. Freire, *Polym. Chem.* **2017**, *8*, 3740.
[40] S. Arias, M. Núñez-Martínez, E. Quiñoá, R. Riguera, F. Freire, *Small* **2017**, *13*, 1602398.
[41] R. Rodríguez, S. Arias, E. Quiñoá, R. Riguera, F. Freire, *Nanoscale* **2017**, *9*, 17752.
[42] F. Freire, J. M. Seco, E. Quiñoá, R. Riguera, *J. Am. Chem. Soc.* **2012**, *134*, 19374.
[43] M. Fernández-Míguez, M. Núñez-Martínez, E. Quiñoá, F. Freire, *ACS Nano* **2024**, *42*, 28822.
[44] M. Núñez-Martínez, M. Fernández-Míguez, E. Quiñoá, F. Freire, *Angew. Chem., Int. Ed.* **2024**, *63*, 202403313.
[45] F. Rey-Tarrío, R. Rodríguez, E. Quiñoá, R. Riguera, F. Freire, *Angew. Chem., Int. Ed.* **2021**, *60*, 8095.
[46] F. Rey-Tarrío, R. Rodríguez, E. Quiñoá, F. Freire, *Nat. Commun.* **2023**, *14*, 1742.
[47] Y. Zhang, Y. Wu, R. Xu, J. Deng, *Polym. Chem.* **2019**, *10*, 2290.
[48] H. Kim, Y. J. Jin, B. S. I. Kim, T. Aoki, G. Kwak, *Macromolecules* **2015**, *48*, 4754.
[49] J. J. Tarrío, R. Rodríguez, B. Fernández, E. Quiñoá, F. Freire, *Angew. Chem., Int. Ed.* **2022**, *61*, 202115070.
[50] J. J. Tarrío, R. Rodríguez, J. Crassous, E. Quiñoá, F. Freire, *Angew. Chem., Int. Ed.* **2023**, *62*, 202307059.
[51] J. Matern, Y. Dorca, L. Sánchez, G. Fernández, *Angew. Chem., Int. Ed.* **2019**, *58*, 16730.
[52] M. Wehner, F. Würthner, *Nat. Rev. Chem.* **2020**, *4*, 38.
[53] J. Matern, Z. Fernández, N. Bäumer, G. Fernández, *Angew. Chem., Int. Ed.* **2022**, *61*, 202203783.
[54] Y. Deng, M. Wang, Y. Zhuang, S. Liu, W. Huang, Q. Zhao, *Light: Sci. Appl.* **2021**, *10*, 76.
[55] H. Tanaka, Y. Inoue, T. Mori, *ChemPhotoChem.* **2018**, *2*, 386.

